Influence of chirality on director configuration and droplet interaction in ferroelectric free-standing films

P. V. Dolganov[1] and P. Cluzeau[2]
[1]*Institute of Solid State Physics, Russian Academy of Sciences, 142432 Moscow Region, Chernogolovka, Russia*
[2]*Université Bordeaux I, CNRS, Centre de Recherche Paul Pascal, Avenue A. Schweitzer, 33600 Pessac, France*
(Received 16 January 2008; published 4 August 2008)

Droplets in smectic free-standing films interact due to elastic distortion of the **c**-director field and formation of topological defects. Our experiments show that chirality of the liquid-crystal medium plays a key role in the interaction between droplets. We find that the configuration of the **c**-director field near the droplets and the position of the topological defects on the droplet boundary depend on droplet size and film polarity. An intermediate **c**-director configuration between dipolar and quadrupolar is formed near droplets in smectic films due to the competition between elasticity and chirality. We observed that the distance between droplets in self-organized structures depends on the position of defects on the droplet boundary and significantly changes with respect to that for dipolar droplets. Our results open the way to modify the droplet interaction and the structures formed by droplets.

DOI: 10.1103/PhysRevE.78.021701 PACS number(s): 61.30.Jf, 61.30.Gd, 81.16.Dn

Self-organization of inclusions in liquid-crystal media and formation of different structures from inclusions are subjects of intensive investigations [1–13]. In recent years, a nontrivial collective behavior of droplets was found in smectic free-standing films [5,6,9–11,13]. The droplets form chains, clusters, and two-dimensional ordered structures [5,6,9–11,13]. The mechanism of interaction between droplets is related to the elastic distortion of the liquid-crystal medium [1–3]. In free-standing films the molecular layers are parallel to the free surfaces. In nonpolar smectic-*C* (Sm*C*) and ferroelectric smectic-*C** (Sm*C**) phases, the long axes of molecules are tilted by a polar angle θ with respect to the layer normal. The in-plane molecular ordering is described by the projection of the long axes of the molecules onto the layer plane, or the so-called **c**-director field [14]. Most investigations of self-organization of inclusions in free-standing films were made with nematic (*N*), cholesteric (*N**), and isotropic (*I*) droplets as inclusions. Tangential or normal anchoring of molecules on the droplet boundary leads to elastic deformation of the **c**-director field and formation of topological defect(s) on the droplet boundary.

Until recently, most theoretical and experimental investigations were made for dipolar and quadrupolar inclusions. However, theory predicts that chirality can essentially modify the position of topological defects on the droplet boundary and lead to a mixed **c**-director configuration near the droplets [15,16].

We find in ferroelectric films a nontrivial dependence of the topological defect position and droplet interaction on droplet size and film polarity. The droplet interaction and the distance between droplets in self-organized structures depend on the position of defects on the droplet boundary and can be sufficiently changed. Our model of the droplet takes into account the structure of the meniscus and the surface layers of the droplet. The experimental results are explained by the competition between quadratic and linear elasticity of the film, meniscus, and surface layers in the droplets.

The experiments were carried out on films of chiral 4′-undecyloxybiphenyl-4-yl 4-(1-methylheptyloxy)benzoate (11BSMHOB) [17], racemic 11BSMHOB, and mixtures of chiral and racemic 11BSMHOB. The latter enabled us to perform the measurements in films with different values of polarization and chirality. The sequence of phase transitions in the bulk sample was SmC^* $\leftrightarrow$ N^* $\leftrightarrow$ I in chiral 11BSMHOB isomer and SmC $\overset{108.2\ ^\circ\mathrm{C}}{\leftrightarrow}$ N $\overset{123.9\ ^\circ\mathrm{C}}{\leftrightarrow}$ I in the racemate. The electric polarization of the chiral isomer is 40 nC/cm^2 [17]. Films were prepared by drawing the liquid crystal in the smectic state across a 4-mm hole in a thin glass plate. Observations were performed in depolarized reflected light microscopy [18] and between crossed polarizers. The images of the droplets and textures in the films were taken with a charge-coupled device camera.

Cholesteric or nematic droplets nucleate with tangential anchoring of the **c** director at the droplet boundary at the temperature T_d near the bulk SmC^*-N^* (or SmC-N) phase transition temperature T_C. The droplet structure depends on temperature. It is known that smectic layers exist near the droplet surface [19–21]. The smectic ordering penetrates into the droplet on the distance of the smectic correlation length ξ. At high temperature ($T>T_d$) ξ is small, $\xi<L/2$, where L is the film thickness. On cooling below T_d the correlation length ξ may become larger than $L/2$.

Figure 1 shows photographs of droplets in films with different polarization. In a film with high chirality [Fig. 1(a), the chiral isomer] the droplets nucleate with one topological defect. The **c**-director field near the droplets has dipolar symmetry [Fig. 1(d)]. A defect with topological charge $S=-1$ localizes on the droplet boundary. In a nonpolar film [Fig. 1(c), racemate, nonchiral film] droplets nucleate with two $S=-1/2$ topological defects on the opposite sides of the droplets and with quadrupolar symmetry of the **c**-director field [Fig. 1(f)]. We found a transition from dipolar to quadrupolar configuration on decreasing the polarity of the film and changing the droplet size. Figure 1(b) shows a droplet in the film with polarization 4 nC/cm^2. The transition occurs via the formation of an intermediate configuration with two $S=-1/2$ topological defects [Figs. 1(b) and 1(e)]. Figure 2

 ©2008 The American Physical Society

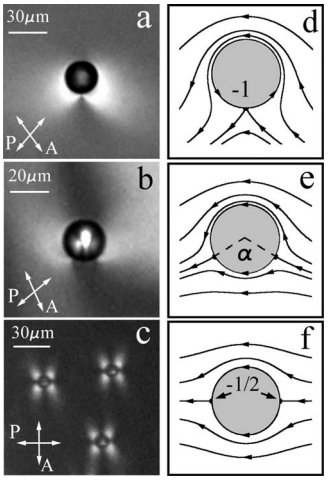

FIG. 1. Droplets in smectic films. (a) A dipolar droplet with an $S=-1$ defect in a film with large polarization (40 nC/cm^2). (b) A droplet with intermediate configuration of the **c**-director field (film with polarization 4 nC/cm^2). (c) Quadrupolar droplets with $S=-1/2$ topological defects on the opposite sides of the droplet (nonpolar film, $\alpha=180°$). The photographs were taken in depolarized reflected light microscopy (a), (b) and between crossed polarizers (c). The orientation of the polarizer (P) and the analyzer (A) is shown in each frame. (d), (e), (f) show schematic representations of the **c**-director field near the droplets.

shows the dependence of the defect angle α between two surface defects seen from the droplet center versus the droplet radius R. The defect angle increases for smaller droplets. In polar films we found quadrupolar droplets at the critical droplet size $R_C \approx 7$ μm. Increase and decrease of R with respect to R_C leads to increase of the dipolar component in the **c**-director configuration near the droplet.

Elastic distortion of the **c**-director field due to quadratic elasticity leads to repulsion between topological defects of the same sign. This is the reason why in nonchiral films two $S=-1/2$ defects are located at the maximum distance from each other, i.e., on the opposite sides of the droplet [quadrupolar configuration, $\alpha=180°$, Figs. 1(c) and 1(f)]. In ferroelectric films attraction between topological defects appears due to the chirality [11]. As a result, in films with high chirality the energetically favorable configuration may be the dipolar configuration with one $S=-1$ defect [$\alpha=0$, Figs. 1(a) and 1(d)]. The competition between the quadratic elasticity of the film and chirality was first studied numerically by Bohley and Stannarius [15]. They showed that this competition may lead to an intermediate position of the topological defects on the droplet boundary ($0<\alpha<180°$). Later, Fukuda found an analytical relation between the defect angle α, droplet size, and chirality, $\tan \alpha/2=\pi/2\lambda R$ [16], where λ is the strength of spontaneous bend [15]. Both calculations [15,16] give a similar dependence of the defect angle on R and λ for the case of uniform **c**-director orientation at infinity. Our experimental results for small droplets (Fig. 2) are not described by the model [15,16]. According to theory [15,16], the quadrupolar configuration should be observed in the limit $R \to 0$. In our experiment, the quadrupolar configuration ($\alpha=180°$) was found for droplets with finite size $R_C \approx 7$ μm. As follows from theory the largest defect angle should be $\alpha=180°$. Meanwhile, we observed droplets with $\alpha>180°$ for $R<R_C$ (Fig. 2).

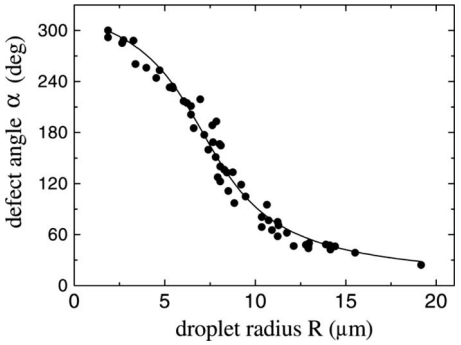

FIG. 2. Solid circles show the dependence of the defect angle α on droplet size R. The solid line is a fit using the Eq. (4) with $H(L_m-2\xi)/(L-2\xi)=7$ μm, $\lambda(L-2\xi)/(L+L_d)=0.5$ μm^{-1}. $T=T_d+0.2$ °C. The measurements were made on films with polarization 4 nC/cm^2.

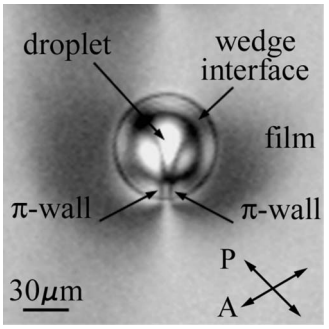

FIG. 3. A cholesteric droplet with a smectic wedge interface in a ferroelectric film. The two dark lines in the wedge are π walls. The photograph was taken in depolarized reflected light microscopy; the orientation of the polarizer (P) and the analyzer (A) is shown in the figure. $T=108.2$ °C. The film was prepared from a mixture of chiral isomer (10 wt %) and racemate. The electric polarization of the film was 4 nC/cm^2.

We explain nontrivial droplet behavior (Fig. 2) by a more complex structure of the droplet than the model of inclusion proposed in Refs. [15,16]. We take into account the surface ordering [19] in the droplet and the structure of the interface (meniscus) between the droplet and the film. The resolution of our optical microscope does not allow observation of the fine structure of the meniscus at high temperature when the size of the meniscus is small. In order to understand the key role of the meniscus and surface smectic ordering in the droplet for the configuration of the **c**-director field and the interparticle interaction, we consider a droplet at low temperature (Fig. 3).

On cooling to T_C the meniscus grows and forms a smectic wedge interface of larger thickness than the film [10]. Figure 3 shows such an interface around the cholesteric droplet. Now the characteristic structure inside the interface between the droplet and the film can be optically resolved. In Fig. 3 two $S=-1/2$ topological defects are located on the outer boundary of the wedge. Inside the wedge $S=-1/2$ defects are replaced by two π walls [10] (dark lines in Fig. 3). The

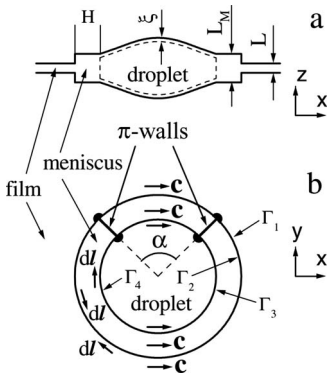

FIG. 4. Schematic representation of the droplet with meniscus in a smectic film. L and L_m are, respectively, the thickness of the film and of the meniscus, and H is the width of the meniscus. ξ is the surface smectic correlation length. Solid points in (b) show the $-1/2$ topological defects on the outer meniscus boundary and on the inner droplet boundary. The two solid lines are π walls.

ring borders impose tangential anchoring on the **c** director in the wedge and in the surface smectic layers of the droplet. The **c** director rotates by π across the π walls. If the wedge size does not significantly exceed the droplet size, the π walls are oriented nearly in the radial direction. We use these observations to develop a model that describes our experimental results quantitatively.

In chiral SmC^* films the free energy F of the system includes the energies of quadratic F_q and linear F_l elasticity $F=F_q+F_l$ [22–24],

$$F_q = \frac{1}{2}K \int [(\nabla \cdot \mathrm{c})^2 + (\nabla \times \mathrm{c})^2] dx\, dy\, dz, \tag{1}$$

$$F_l = \frac{1}{2}K \int [\lambda \cdot (\nabla \times \mathrm{c})]_z dx\, dy\, dz. \tag{2}$$

We assume equal splay (K_S) and bend (K_B) curvature elastic constants ($K_B=K_S=K$). The elastic constant λ depends on the chirality of the sample.

A schematic representation of the droplet with meniscus is shown in Fig. 4. The free energy F_l is a total derivative and can be expressed as an integral over the boundaries of the film, the meniscus, and the droplet, $F_l=\frac{1}{2}K\lambda\int_\Gamma \mathbf{c}\cdot d\mathbf{l}\, dz$, where vector $d\mathbf{l}$ is parallel to the boundaries of the droplet and the meniscus, $\Gamma=\Gamma_1+\Gamma_2+\Gamma_3+\Gamma_4$ (Fig. 4). Γ_1 and Γ_2 are the outer and inner contours over the boundary between the film and the meniscus; Γ_3 and Γ_4 are the outer and inner contours of the droplet. Different thicknesses of the smectic on the two sides of the boundaries between the film and the meniscus and between the meniscus and the droplet lead to a nonzero value F_l after integration over the inner and outer contours. We consider the case of uniform orientation of the **c** director at infinity, i.e., the integral over the outer boundary of the film is independent of α [15,16]. After integration over Γ and z, we obtain

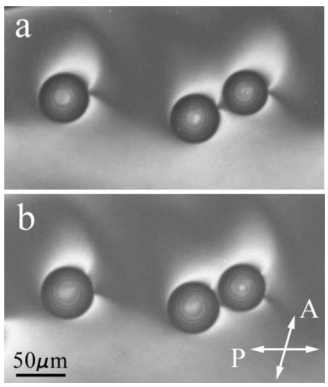

FIG. 5. At low temperature the droplets in a film with high chirality are dipolar (a). On heating the distance between defects increases, $T=T_d+0.4$ °C (b). The increase of the defect angle in the droplets leads to decrease of the distance between droplets. The photograph was taken in depolarized reflected light microscopy; the orientation of the polarizer (P) and the analyzer (A) is shown in (b). Polarization of the film was 40 nC/cm^2.

$$F_l = K\lambda[(RL - HL_m) - 2\xi(R - H)](\alpha - \pi), \tag{3}$$

where R is the radius of the droplet with the meniscus, L_m is the thickness of the meniscus, and H is its width. In reality the thickness of the meniscus is not constant. For simplicity we assume the meniscus to be steplike (Fig. 4). L_m stands for the average thickness of the meniscus. The presence of the surface smectic layers and the meniscus leads to a more complex expression of F_l with respect to previous models [16]. In our model we do not take into account the linear elasticity of the cholesteric phase inside the droplet, since $\lambda=0$ for the cholesteric phase. The linear elasticity describing the cholesteric twist does not depend on α in our model of the droplet.

The energy of quadratic elasticity F_q consists of three terms, $F_q=F_q^f+F_q^m+F_q^d$, which describe the energy of the film F_q^f, the meniscus F_q^m, and the droplet F_q^d. Since the **c**-director orientation is circular both inside and outside the angle α, F_q^m does not depend on the position of the π walls, that is, on α. The energy F_q^f has the form $F_q^f=-\pi KL \ln \sin(\alpha/2)$ [16]. The surface smectic layers orient the molecules of the cholesteric phase inside the droplets. The elastic constant for the cholesteric is approximately the same as for smectic, so $F_q^d=-\pi KL_d \ln \sin(\alpha/2)$, where L_d is the average droplet thickness. Taking F_l from (3), the minimization of the total free energy $F=F_q+F_l$ gives

$$\tan\frac{\alpha}{2} = \frac{\pi(L+L_d)}{2\lambda[R(L-2\xi) - H(L_m-2\xi)]}. \tag{4}$$

The experimental data are well fitted by Eq. (4) with $H(L_m-2\xi)/(L-2\xi)=7$ μm, $\lambda(L-2\xi)/(L+L_d)=0.5$ μm^{-1} (the solid curve in Fig. 2). So the meniscus and the surface layers of the droplet play a key role in the position of the topological defects. Due to chirality the energy of the **c** director and (4) are not symmetric with respect to the quadrupolar configuration ($\alpha=180°$).

We have so far considered the change of the defect angle α with droplet size. However, according to our model the

defect angle α depends also on ξ. We found that above the bulk transition temperature the defect angle depends on temperature [Figs. 5(a) and 5(b), the left droplet]. By changing temperature, the defect angle could be changed from $\alpha=0$ to $\alpha=360°$. In our opinion, this change of α is related to the change of ξ. It is known that the surface correlation length decreases with increasing temperature, which should lead according to (4) to a change of α.

The interaction of the droplets at both large and small distances depends on α. At large distance, the interaction between droplets is determined by the topological dipole moment [2] of the droplet and defects. Its value, $2R\cos(\alpha/2)$, decreases with increasing α and changes sign at $\alpha=\pi$. Figure 5 (two right droplets) demonstrates the change of the interaction between droplets at small distance. The distance between droplet boundaries in a chain decreases with increasing defect separation (Fig. 5). With changing temperature the distance between droplets in chains changes by a factor of more than 3.

In summary, chirality plays an important role in interaction and self-organization of inclusions in liquid crystals. In smectic films the interaction and the distance between droplets in self-organized structures change drastically with chirality and droplet size. By preparing the SmC^* films with different chirality, we observed a transition between dipolar and quadrupolar droplets. The competition between quadratic elasticity of the film and chirality leads to formation of intermediate configurations of the **c**-director field between dipolar and quadrupolar. The possibility of changing the defect angle between topological defects opens the way for manipulating the structures formed by inclusions in polar films.

This work was supported by INTAS Grant No. 06-1000014-6462, Grant No. MK-2382.2007.2, and by the Russian Science Support Foundation. We thank A. Babeau and S. Gineste for the synthesis of the liquid crystals.

[1] P. Poulin, H. Stark, T. C. Lubensky, and D. A. Weitz, Science **275**, 1770 (1997).
[2] D. Pettey, T. C. Lubensky, and D. R. Link, Liq. Cryst. **25**, 579 (1998).
[3] J.-C. Loudet, P. Barois, and P. Poulin, Nature (London) **407**, 611 (2000).
[4] V. G. Nazarenko, A. B. Nych, and B. I. Lev, Phys. Rev. Lett. **87**, 075504 (2001).
[5] P. Cluzeau, P. Poulin, G. Joly, and H. T. Nguyen, Phys. Rev. E **63**, 031702 (2001).
[6] P. Cluzeau, G. Joly, H. T. Nguyen, and V. K. Dolganov, Pis'ma Zh. Eksp. Teor. Fiz. **76**, 411 (2002) [JETP Lett. **76**, 351 (2002)].
[7] P. Patrício, M. Tasinkevych, and M. M. Telo da Gama, Eur. Phys. J. E **7**, 117 (2002).
[8] M. Tasinkevych, N. M. Silvestre, P. Patrício, and M. M. Telo da Gama, Eur. Phys. J. E **9**, 341 (2002).
[9] P. V. Dolganov, E. I. Demikhov, V. K. Dolganov, B. M. Bolotin, and K. Krohn, Eur. Phys. J. E **12**, 593 (2003).
[10] C. Völtz and R. Stannarius, Phys. Rev. E **70**, 061702 (2004).
[11] P. V. Dolganov, H. T. Nguyen, G. Joly, V. K. Dolganov, and P. Cluzeau, Europhys. Lett. **76**, 250 (2006).
[12] J. Kotar, M. Vilfan, N. Osterman, D. Babič, M. Čopič, and I. Poberaj, Phys. Rev. Lett. **96**, 207801 (2006).
[13] P. V. Dolganov, H. T. Nguyen, E. I. Kats, V. K. Dolganov, and P. Cluzeau, Phys. Rev. E **75**, 031706 (2007).
[14] P. G. de Gennes and J. Prost, *The Physics of Liquid Crystals*, 2nd ed. (Clarendon Press, Oxford, 1993).
[15] C. Bohley and R. Stannarius, Eur. Phys. J. E **23**, 25 (2007).
[16] J. Fukuda, Eur. Phys. J. E **24**, 91 (2007).
[17] P. Cluzeau, M. Ismaili, A. Annakar, M. Foulon, A. Babeau, and H. T. Nguyen, Mol. Cryst. Liq. Cryst. Sci. Technol., Sect. A **362**, 185 (2001).
[18] D. R. Link, G. Natale, R. Shao, J. E. Maclennan, N. A. Clark, E. Korblova, and D. M. Walba, Science **278**, 1924 (1997).
[19] B. M. Ocko, A. Braslau, P. S. Pershan, J. Als-Nielsen, and M. Deutsch, Phys. Rev. Lett. **57**, 94 (1986).
[20] P. V. Dolganov, P. Cluzeau, G. Joly, V. K. Dolganov, and H. T. Nguyen, Phys. Rev. E **72**, 031713 (2005).
[21] P. V. Dolganov, H. T. Nguyen, G. Joly, V. K. Dolganov, and P. Cluzeau, Europhys. Lett. **78**, 66001 (2007).
[22] S. A. Langer and J. P. Sethna, Phys. Rev. A **34**, 5035 (1986).
[23] I. Kraus and R. B. Meyer, Phys. Rev. Lett. **82**, 3815 (1999).
[24] R. D. Kamien and J. V. Selinger, J. Phys.: Condens. Matter **13**, R1 (2001).